Asian Journal of Chemistry; Vol. 34, No. 11 (2022), 2915-2921

ASIAN JOURNAL OF CHEMISTRY

https://doi.org/10.14233/ajchem.2022.23934

Palladium(II) Complexes with *S*-Benzyl Dithiocarbazate: Synthesis, Characterization *in vitro* Antimicrobial and Anticancer Activities

AKSHITA JAIN[1], RAMHARI MEENA[1], NAVEEN SHARMA[1], SAVITA BELWAL[2] and NIGHAT FAHMI[1,*]

[1]Department of Chemistry, University of Rajasthan, Jaipur-302004, India
[2]Department of Chemistry, Anurag University, Hyderabad-500088, India

*Corresponding author: E-mail: nighat.fahmi@gmail.com

Received: 25 May 2022; *Accepted*: 19 August 2022; *Published online*: 19 October 2022; AJC-21006

Square planar complexes of palladium(II) were prepared by the reaction of $PdCl_2$ with four different thio Schiff bases, namely 2-acetylpyridine S-benzyl dithiocarbazate (L^1H), 2-acetylthiophene-*S*-benzyl dithiocarbazate (L^2H), 2-acetylfuran-*S*-benzyl dithiocarbazate (L^3H) and 2- acetylnaphthalene-*S*-benzyl dithiocarbazate (L^4H) in a 1:2 molar ratio. Elemental analysis, molecular weight determinations, conductance measurements and spectral data, including electronic, IR, ^1H and ^{13}C NMR and X-ray powder diffraction studies, confirmed the formation of palladium(II) complexes. The electrochemical behaviour of one of the palladium(II) complex has also been determined by cyclic voltammetry. The antimicrobial activities of the Schiff base ligands and their corresponding palladium(II) complexes have been tested *in vitro* against various pathogenic bacterial and fungal strains. The cytotoxicity of $[Pd(L^1)_2]$ complex shows the promising results when analyzed using MTT cell proliferation assay.

Keywords: *S*-Benzyldithiocarbazate, Spectral studies, Antimicrobial activity, Cytotoxicity.

INTRODUCTION

Schiff bases are structurally diversified and have gained the attention of many scientists worldwide due to their multiple facet applications [1-4]. Transition metal complexes of Schiff bases grew enormously and encompassed a wide and diverse range of subjects and aspects of biocoordination chemistry [5-10]. The design and synthesis of the symmetrical Schiff bases, as well as their metal(II) complexes, have been of interest because they are easy to make, have a wide range of structures and can be changed to make them more or less reactive [11]. Metal complexes of sulfur-nitrogen chelating ligands have attracted attention due to their physico-chemical, pharmacological and chemotherapeutic properties [12-15].

The physico-chemical, pharmacological and chemotherapeutic properties have stimulated interest in metal complexes of sulfur-nitrogen chelating agents especially those formed from *S*-benzyl esters of dithiocarbazoic acid [16]. The biological effects and toxicology of the coordination complexes of palladium and platinum complexes, as their requirements in pharmacological activities, are the areas of increasing research interest [17,18]. Biological properties such as anticancer [19], antitumor [20], *etc*. exhibited by Pd(II) and Pt(II) metals revealed their dynamic nature [21,22]. Furthermore, in view of the enlarged chelating behaviour of *S*-benzyldithiocarbazates, as well as biological importance of palladium complexes, it has been considered worthwhile to synthesize, characterize some new palladium(II) derivatives of *S*-benzyldithiocarbazates and to investigate their physico-chemical and structural features as well as the biological activity.

EXPERIMENTAL

Palladium(II) chloride was obtained from Alfa Aesar and used as received. The rast camphor approach was applied to determine the molecular weight of newly synthesized compounds [23]. A Systronics model 305 conductivity bridge was used to assess conductivity. The ^1H & ^{13}C NMR spectra were recorded on a JEOL-ECS-400 NMR spectrophotometer using DMSO-d_6 as solvent. The UV-vis spectra were acquired using an LAMBDA-750 spectrophotometer. The IR spectra were recorded on a Nicolet Megna FTIR-550 spectrometer using KBr pellets in the range of 4000-400 cm^{-1}.

Synthesis of Schiff base ligands: Ligands, L^1H, L^2H, L^3H and L^4H were synthesized by the condensation of *S*-benzyldithiocarbazate with 2-acetylpyridine, 2-acetylthiophene, 2-acetylfuran and 2-acetylnaphthalene in ethanol, respectively (**Scheme-I**). The reaction mixtures were allowed to be heated under reflux for about 4-5 h and then cooled. The white or yellow crystalline precipitates were obtained from the solution, which was concentrated under reduced pressure. These resulting solid compounds were recrystallized twice in alcohol.

Synthesis of Pd(II) complexes of $[Pd(L^{1-4})_2]$ type: The $PdCl_2$ was dissolved in methanol and mixed separately with a methanolic solution of ligands in 1:2 molar ratio. Then an aqueous solution of ammonia was added to adjust the alkaline pH of the reaction mixture and then heated the reaction mixture under reflux for about 1 h. The resulting solids were isolated and washed with MeOH and dried *via* vacuum.

Synthesis of Pd(II) metal complexes of $[Pd(L^{1-4}H)_2]Cl_2$ type: The methanolic solutions of $PdCl_2$ and the corresponding ligands were mixed in 1:2 molar ratio. The reaction mixtures were stirred for 2-3 h in the presence of a few drops of conc. HCl. The resulting products were recovered by filtrations, washed with methanol and then dried in vacuum.

Antifungal studies: The ligands and their complexes were tested for antifungal activity against two pathogenic fungi, *Penicillin cryogens* and *Rhizoctonia phaseoli* on Czapek's agar medium [24]. The required amounts of the compounds dissolved in methanol were added to this medium in order to achieve the desired concentrations (0.01% and 0.1%). The medium was then placed into petri dishes and fungus spores were inoculated onto them. The controls were also performed concurrently, with three replicates in each example. The fungus' linear growth was measured by measuring the diameter of the fungal colony after 96 h and the % inhibition was calculated using eqn. 1:

$$\text{Inhibition (\%)} = \frac{C - T}{C} \times 100 \quad (1)$$

where C and T are the diameters of the fungal colony in the control and the test plates after four days, respectively.

Antibacterial activity: For the evaluation of degree of inhibitory effects on the growth of a wide spectrum of microorganisms, antibacterial activity was performed against two bacteria including Gram-positive (*Bacillus subtilis*) and Gram-negative (*Pseudomonas aeruginosa*). The antibacterial activities of newly synthesized complexes were evaluated by the paper disc plate method" using the inhibition zone technique [25]. The reference drug used was tetracyclin. All the compounds were dissolved in methanol in different concentrations (100 and 500 ppm). The inhibition zone around each disc was measured (mm) after 24-30 h.

Anticancer activity: DMEM (Dulbecco's modified Eagles medium), MTT [3-(4,5-dimethylthiazol-2-yl)-2,5-diphenyl tetrazolium bromide], trypsin and EDTA phosphate buffered saline (PBS) were obtained from Sigma Chemicals Co. (USA) and fetal bovine serum (FBS) were purchased from Gibco. The MTT cell proliferation assay was used to assess the anticancer activity of the synthesized Pd(II) complex. The MTT cell multiplication assay evaluates the rate of cell proliferation and, conversely, the reduction in cell viability caused by metabolic processes such as apoptosis or necrosis.

Maintenance of cell line: MCF-7 breast adenocarcinoma cancer cell line was obtained from NCCS, Pune, India and were maintained in MEM supplemented with 10% FBS and the antibiotics penicillin/streptomycin (0.5 mL) in a 5% CO_2/95% air environment at 37 ºC.

Procedure: The MTT assay was used to assess cell viability in three independent trials with six concentrations of chemical in triplicate. On a microplate reader, the optical density of solubilized crystals in DMSO was determined at 570 nm. The percentage growth inhibition was determined using the following method and the concentration of test drug required to inhibit cell growth by 50%. Data were obtained

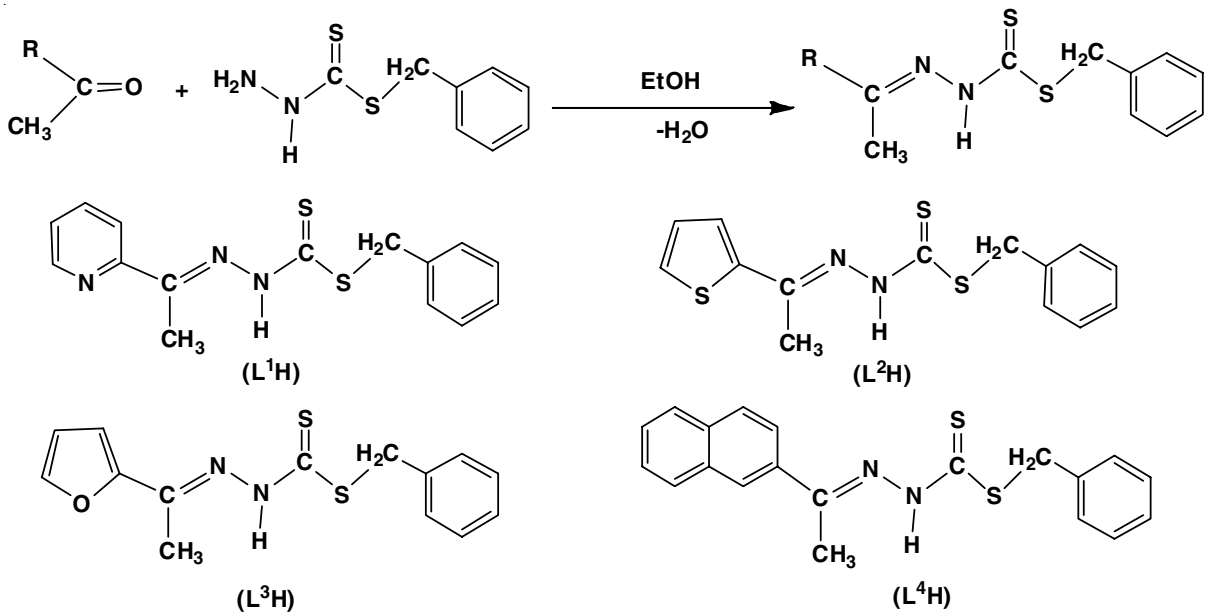

Scheme-I: Synthetic scheme of the ligands L^1H, L^2H, L^3H and L^4H

using origin software from the dose response curves for each cell line [20,21].

$$\text{Inhibition (\%)} = \frac{100\ (\text{Control} - \text{Treatment})}{\text{Control}}$$

RESULTS AND DISCUSSION

As predicted by analytical data, metal salts reacted with ligands in a 1:2 (M:L) molar ratio to yield complexes of general compositions, $[(Pd(LH)_2)]Cl_2$ and $[(Pd(L)_2]$. The interaction of metal chloride with the ligands in the presence of few drops of conc. HCl results in the formation of the type $[(Pd(LH)_2)Cl_2]$ complexes. When reactions were carried out in the presence of aqueous NH_4OH, however, complexes of the type $[(Pd(L)_2)]$ were formed. The reactions can be represented as follows:

$$PdCl_2 + 2L^{1\text{-}4}H + 2NH_4OH \longrightarrow [Pd(L^{1\text{-}4})_2] + 2NH_4Cl + 2H_2O$$

$$PdCl_2 + 2L^{1\text{-}4}H \longrightarrow [Pd(L^{1\text{-}4}H)_2]Cl_2$$

where, LH is the Schiff base ligands.

The molecular weight determinations of the resulting coloured complexes revealed the monomeric character of the complexes (Table-1). All the Pd(II) complexes were soluble in DMSO, DMF and $CHCl_3$. The non-electrolytic behaviour of $[Pd(L)_2]$ complexes is corroborated by their molar conductance values in 10^{-3} M solutions, which are in the 13-15 ohm^{-1} cm^2 mol^{-1} range. The $[(Pd(LH)_2)]$ Cl_2 complexes, on the other hand, were 1:2 electrolytes with conductance values ranging from 215-224 ohm^{-1} cm^2 mol^{-1}.

Electronic spectra: The electronic spectra of Pd(II) complexes recorded in distilled DMSO solvent provided the evidence for their square planar shape. The metal complexes' electronic spectra show three spin permitted *d-d* transitions, namely $^1A_{1g} \rightarrow {}^1A_{2g}$, $^1A_1g \rightarrow {}^1B_1g$ and $^1A_1g \rightarrow {}^1E_1g$, which occur from the lower lying *d* orbital to the empty $d_{x^2-y^2}$ orbital. The ground state is ^1A_1g, while the excited states corresponding to the aforementioned transition are, in increasing energy order, ^1A_2g, ^1B_1g and ^1E_1g. The *d-d* transition bands can be seen at 519-525, 455-480 and 440-451 nm. Three orbital parameters, Δ_1, Δ_2 and Δ_3 were calculated using a Slater-Condon inter-electronic repulsion parameter of $F_2 = 10$ and $F_4 = 600$ cm^{-1}. The ν_2/ν_1 values calculated in Table-2 are extremely close to the reported values for the square planar geometry [26].

IR spectra: By examining the prominent IR bands of the ligands and their palladium(II) complexes, the mode of ligand-metal coordination has been established. The IR spectra show free ligand bands attributable to ν(C=N) and ν(C=S) at 1622-1615 cm^{-1} and 1032-1024 cm^{-1}, respectively. Due to the ν(NH) vibrations, ligands have strong bands in the 3355-3245 cm^{-1} range. A doublet at 2900-2960 cm^{-1} has been assigned to symmetric and asymmetric vibrations of the S-CH_2-C_6H_5 grouping. Several changes in the ligand bands during complexation suggest coordination *via* the azomethine nitrogen and sulphur of the thiolic form of the ligands. The complexes missing the ν(NH) absorption bands, indicating ligand enolization followed by deprotonation during complexation to the metal atom and the ν(C=N) bands in complexes appear at 1600-1598 cm^{-1}, which is signi-ficantly lower than the free ligand values, indicating coordi-nation by the azomethine nitrogen atoms of the Schiff bases. The doublet of S-CH_2-C_6H_5 is reduced to a weak doublet. Aside from these, coordination shifts the ν(N-N) and ν(C=S) modes to a lower frequency. Several new bands in the spectra of metal complexes in the region, 454-398 cm^{-1} and 384-310

TABLE-1
PHYSICAL PROPERTIES AND ANALYTICAL DATA OF THE LIGANDS AND THEIR CORRESPONDING PALLADIUM(II) COMPLEXES

Compound	Colour	m.p. (°C)	Elemental analysis (%): Found (calcd.)						m.w. found (calcd.)
			C	H	N	S	Cl	Pd	
L^1H	Brown	148	59.68 (59.77)	4.98 (5.01)	13.76 (13.94)	21.19 (21.27)	–	–	289.06 (301.42)
L^2H	White	102	54.80 (54.89)	4.46 (4.60)	9.05 (9.14)	31.34 (31.40)	–	–	286.96 (306.32)
L^3H	Light brown	140	57.82 (57.90)	4.74 (4.80)	9.51 (9.64)	21.85 (22.08)	–	–	249.50 (290.50)
L^4H	Brown	118	68.49 (68.53)	5.08 (5.17)	7.54 (7.99)	18.14 (18.29)	–	–	334.85 (350.50)
$[Pd(L^1H)_2]Cl_2$	Brown	260	46.08 (46.18)	3.80 (3.87)	10.76 (10.77)	8.06 (8.12)	8.94 (9.08)	13.60 (13.64)	746.87 (780.17)
$[Pd(L^1)_2]$	Brown	208	50.87 (50.94)	4.23 (4.27)	11.84 (11.87)	9.00 (9.06)	–	15.00 (15.04)	697.13 (707.24)
$[Pd(L^2H)_2]Cl_2$	Brown	300 (d)	42.49 (42.57)	3.52 (3.57)	7.00 (7.09)	16.29 (16.32)	8.85 (8.97)	13.41 (13.47)	763.90 (789.97)
$[Pd(L^2)_2]$	Brown	170	46.80 (46.89)	3.87 (3.93)	7.76 (7.81)	17.86 (17.88)	–	14.80 (14.83)	698.45 (717.14)
$[Pd(L^3H)_2]Cl_2$	Brown	178	44.25 (44.34)	3.68 (3.72)	7.36 (7.38)	8.42 (8.45)	9.28 (9.35)	14.96 (14.03)	738.15 (758.23)
$[Pd(L^3)_2]$	Brown	300 (d)	48.96 (49.07)	4.06 (4.11)	8.09 (8.17)	9.30 (9.35)	–	15.48 (15.52)	669.08 (685.30)
$[Pd(L^4H)_2]Cl_2$	Brown	230	54.64 (54.69)	4.08 (4.13)	6.30 (6.37)	7.26 (7.300	7.97 (8.07)	12.08 (12.11)	856.23 (878.33)
$[Pd(L^4)_2]$	Brown	280 (d)	59.57 (59.65)	4.47 (4.50)	6.93 (6.95)	7.95 (7.96)	–	13.18 (13.21)	784.12 (805.40)

TABLE-2
ELECTRONIC SPECTRAL DATA OF THE LIGANDS AND THEIR PALLADIUM(II) COMPLEXES

Complexes	Transition	Spectral bands (cm^{-1})	Δ_1	Δ_2	Δ_3	ν_1/ν_2
$[Pd(L^1H)_2]Cl_2$	$^1A_{1g}\rightarrow{}^1A_{2g}(\nu_1)$	22222	24322	3016	3286	1.09
	$^1A_{1g}\rightarrow{}^1B_{1g}(\nu_2)$	24038				
	$^1A_{1g}\rightarrow{}^1E_{1g}(\nu_3)$	27624				
$[Pd(L^2)_2]$	$^1A_{1g}\rightarrow{}^1A_{2g}(\nu_1)$	20618	22718	4405	3199	1.16
	$^1A_{1g}\rightarrow{}^1B_{1g}(\nu_2)$	23923				
	$^1A_{1g}\rightarrow{}^1E_{1g}(\nu_3)$	27322				
$[Pd(L^3H)_2]Cl_2$	$^1A_{1g}\rightarrow{}^1A_{2g}(\nu_1)$	20833	22933	4176	3064	1.14
	$^1A_{1g}\rightarrow{}^1B_{1g}(\nu_2)$	23809				
	$^1A_{1g}\rightarrow{}^1E_{1g}(\nu_3)$	27173				
$[Pd(L^4)_2]$	$^1A_{1g}\rightarrow{}^1A_{2g}(\nu_1)$	20703	22804	4025	3198	1.13
	$^1A_{1g}\rightarrow{}^1B_{1g}(\nu_2)$	23529				
	$^1A_{1g}\rightarrow{}^1E_{1g}(\nu_3)$	27027				

cm^{-1}, may be assigned to ν(Pd→N) and ν(Pd-S), respectively, based on the suggested coordination in these complexes.

^{1}H NMR spectra: The bonding pattern has been further supported by the ^{1}H NMR spectral data of the ligands and their corresponding palladium complexes, which were recorded in DMSO-d_6 taking TMS as an internal standard. The ^{1}H NMR spectra of the ligands exhibit S-CH_2- proton signals at δ 4.15-4.18 ppm and aromatic protons signals at δ 6.48-7.06 ppm and these remain at the same position in the spectra of the metal complexes. The chelation of the ligand moiety to metal with the sulphur atom has been favoured by the presence of signal at δ 10.04-10.08 ppm due to the proton of –NH group of the ligand, which is absent in the spectra of metal complexes.

^{13}C NMR spectra: ^{13}C NMR data for all four ligands and their Pd(II) complexes have been examined and these spectra confirmed the acceptability of the proposed structures. The carbon atoms connected to the thiolic and azomethine groups in the ligands display signals at δ 174.20-178.10 ppm and δ 160.85-164.70 ppm, respectively. However, these appear in the spectra of the corresponding palladium complexes at δ 160.15-164.42 ppm (thiolic group) and δ 156.25-158.00 ppm (azomethine group). The carbon connected to S and N shows that sulphur and nitrogen atoms play a significant role in the coordination of other atoms.

XRD studies: X-ray powder diffraction studies have been used to deduce the possible lattice dynamics of the finely powdered products *viz.* $[(Pd(L^3H)_2)]Cl_2$ and $[(Pd(L^3)_2)]$. The studies revealed the interplanar spacing values ('*d*' in Å) from the diffractogram of the compounds and the miller indices *hkl* have been assigned to each *d*-value and 2θ angles are reported in Table-3. The results show that the complex belongs to the "orthorhombic" crystal system having unit cells parameters as: a = 21.712 Å, *b* = 35.317 Å and *c* = 6.702 Å for $[(Pd(L^3H)_2)]$-Cl_2 and *a* = 25.58 Å, *b* = 17.040 Å and *c* = 10.644 Å for $(Pd(L^3)_2)$ complex.

Electrochemical studies: The cyclic voltammetric technique on HMDE was employed to study the electrochemical behaviour of $[(Pd(L^2)_2)]$. The compound in the non-aqueous solution gave two distinct peaks at -0.18 V and -0.70 mV (Fig. 1a) which are attributed to the reduction of Pd(II) at HMDE. First peak appears on account of one electron transfer resulting in reduction of Pd(II) to Pd(I) and second peak appears corresponding to anoter one electron transfer step during which Pd(I) undergoes a further reduction to form Pd(0). The peak could be observed in anodic direction of the reverse scans suggesting the irreversible nature of the electrode process (Fig. 1b) and with increase in scan rate, the peak potential shifts towards more negative value.

TABLE-3
X-RAY SPECTRAL DATA OF $[Pd(L^3H)_2]Cl_2$ AND $[(Pd(L^3)_2)]$

$[Pd(L^3H)_2]Cl_2$					$[(Pd(L^3)_2)]$				
h	k	L	2θ	d (Å)	h	k	L	2θ	d (Å)
3	2	0	13.2	6.7017	0	0	1	8.3	10.644
0	3	1	15.2	5.8241	1	0	1	9.0	9.8172
3	1	1	18.2	4.8703	0	1	1	9.6	9.2050
5	1	0	20.6	4.3080	1	1	1	10.8	8.1847
3	5	1	22.0	4.0369	0	0	2	16.8	5.2727
1	9	0	23.1	3.8471	0	1	2	17.3	5.1214
5	5	0	24.1	3.6897	1	1	2	17.9	4.9511
5	4	1	26.4	3.3732	0	2	2	19.7	4.5025
6	0	1	27.9	3.1952	2	2	2	20.6	4.5025
7	5	0	31.5	2.8377	2	1	3	25.6	3.4766
6	7	1	33.2	2.6969	0	1	3	26.3	3.3857
8	0	1	35.6	2.5198	1	3	3	29.6	3.0153
3	5	0	40.2	2.2414	1	3	3	30.2	2.9567
6	8	2	12.1	2.1445	2	3	3	30.8	2.9005
7	9	0	46.1	1.9673	3	3	3	31.4	2.8464

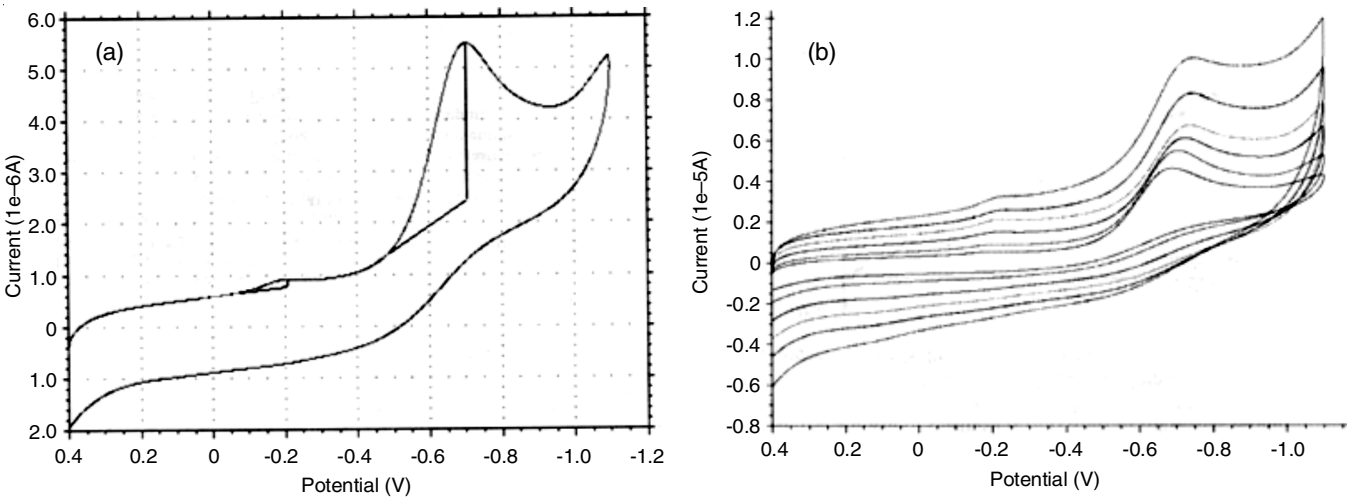

Fig. 1. Cyclic voltammogram of $[Pd(L^2)_2]$ (a) at scan rate 100 mV s^{-1} (b) at different scan rates 50 to 500 mV s^{-1}

Under the aforementioned experimental settings, the influence of scan rate ($\nu^{1/2}$) on stripping peak current (i_p) was also investigated (Fig. 2a-b). The peak potential moved cathodically and the peak current increased steadily as the sweep rate was raised from 50-500 mV/s at a given concentration (3×10^{-3} M). When i_p was plotted against $\nu^{1/2}$, a straight line is obtained, which may be described by the equation.

For first reduction peak

$Y(i_p) = 0.1105\ \nu^{1/2}$ (mV/s) – 0.0625 (μA), $R^2 = 0.9963$

For second reduction peak

$Y(i_p) = 0.0442\ \nu^{1/2}$ (mV/s) – 1.0022 (ÅA), $R^2 = 0.9985$

All these facts pointed towards the diffusion controlled nature of the electrode process. Thus, on the basis of spectral properties mentioned above as well as the analytical results, the square planar geometries for Pd(II) complexes have been proposed (Fig. 3).

Antimicrobial screening: According to the biological screening findings, all the synthesized palladium complexes have higher activity than the ligands but slightly lower than the standard drug (Figs. 4 and 5).

Cytotoxic activity of $[Pd(L^1)_2]$ complex: The cytotoxic activity of only one complex $[Pd(L^1)_2]$ was studied against the

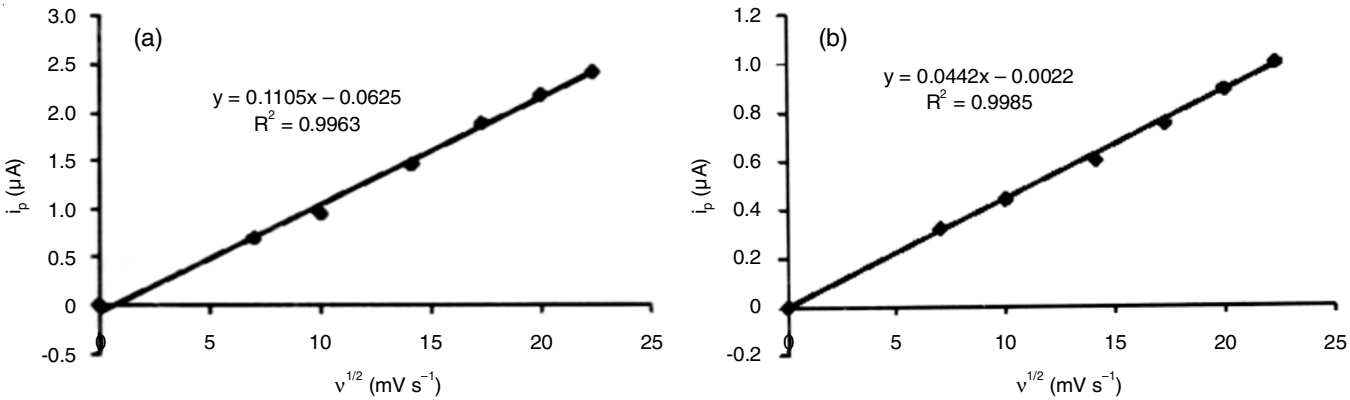

Fig. 2. Plot of peak current *vs*. scan rate for (a) first reduction peak of $[Pd(L^2)_2]$ and (b) second reduction peak of $[Pd(L^2)_2]$

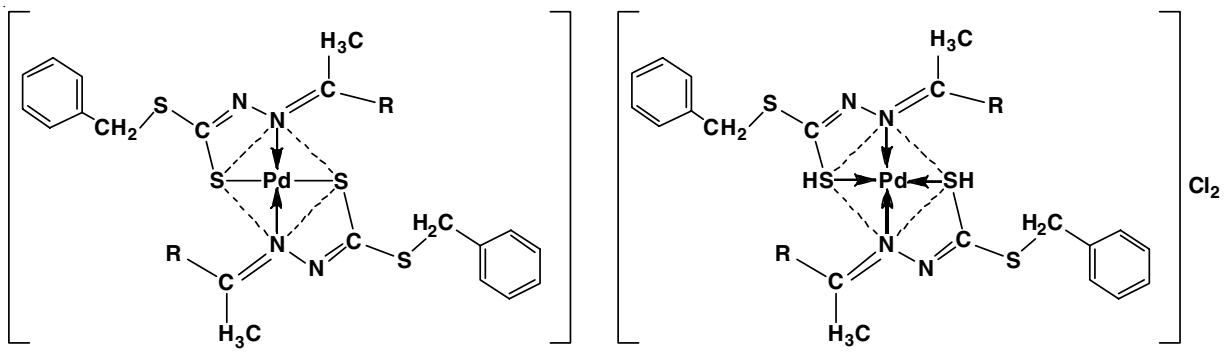

Fig. 3. Proposed square planar geometries for Pd(II) complexes

TABLE-4
CYTOTOXIC PROPERTIES OF PALLADIUM(II) COMPLEX ON MCF 7 CELL LINE

Concentration (µg/mL)	Absorbance at 570 nm			Average	Average-blank	Viability (%)	IC_{50} (µg/mL)
100	0.834	0.837	0.839	0.836	0.8214	34.947	62.73
75	1.196	1.198	1.199	1.197	1.1824	50.306	
50	1.245	1.246	1.248	1.246	1.2314	52.391	
25	1.472	1.476	1.479	1.475	1.4604	62.134	
10	1.597	1.599	1.601	1.599	1.5844	67.41	
5	1.693	1.696	1.699	1.696	1.6814	71.536	
Untreated	2.365	2.365	2.366	2.365	2.3504	100	
Blank	0.003	0.038	0.003	0.0146	0	–	

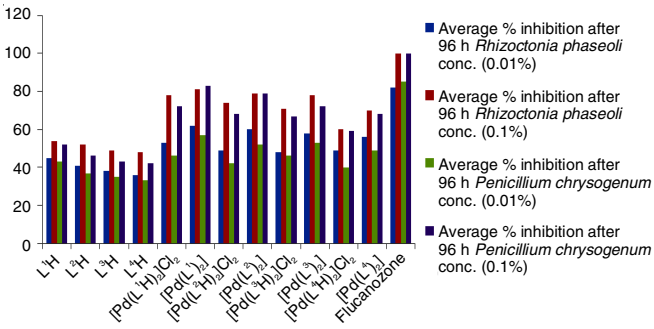

Fig. 4. Fungicidal screening data of the ligands and their palladium(II) complexes

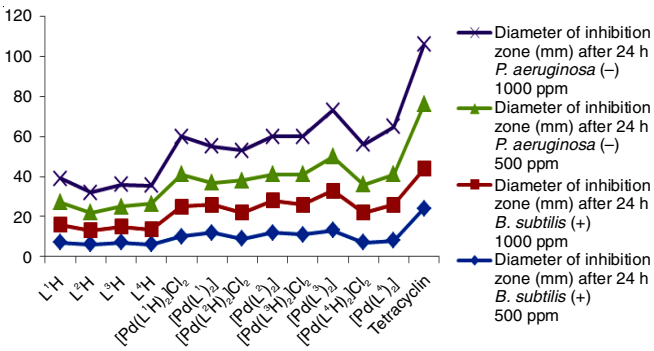

Fig. 5. Antibacterial bioassay results for the ligands and their palladium(II) complexes

MCF-7 breast adenocarcinoma cancer cell line, which proved that capability of arresting tumour growth with an IC_{50} value of 62.73 µg/mL and could be examined further as a possible anticancer agent. Fig. 6 and Table-4 shows the cytotoxic characteristics of $[Pd(L^1)_2]$ complex on the MCF-7 cell line.

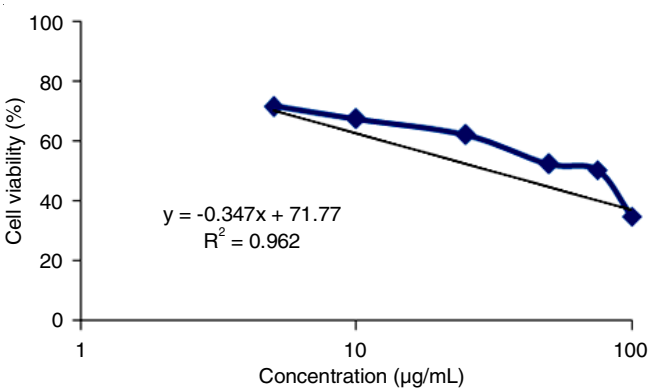

Fig. 6. Cytotoxic effect of the palladium(II) complex on MCF 7 cell line

Conclusion

A biologically relevant ligands and its Pd(II) complexes were synthesized and characterized. The square planar geometries for Pd(II) complexes have been proposed based on the aforesaid spectrum properties as well as the analytical results. Based on the antimicrobial results, all the synthesized Pd(II) complexes will have somewhat higher activity than the ligands but slightly lower activity than the conventional medication. As a result of their broad spectrum nature, they have the potential to become a new antimicrobial agent following further biological research. Furthermore, complexes have the capacity to halt tumour growth in the MCF-7 breast adenocarcinoma cancer cell line.

ACKNOWLEDGEMENTS

One the authors, AJ is thankful to CSIR-University Grant Commission (09/149/2020), New Delhi, India for financial assistance and Dr. B. Lal for conducting the biological studies.

CONFLICT OF INTEREST

The authors declare that there is no conflict of interests regarding the publication of this article.

REFERENCES

1. B.T. Vhanale, N.J. Deshmukh and A.T. Shinde, *Heliyon*, **5**, e02774 (2019); https://doi.org/10.1016/j.heliyon.2019.e02774
2. S. Arroudj, M. Bouchouit, K. Bouchouit, A. Bouraiou, L. Messaadia, B. Kulyk, V. Figa, S. Bouacida, Z. Sofiani and S. Taboukhat, *Opt. Mater.*, **56**, 116 (2016); https://doi.org/10.1016/j.optmat.2015.12.046
3. D. Nartop, E.H. Ozkan, M. Gundem, S. Çeker, G. Agar, H. Ogutcu and N. Sarý, *J. Mol. Struct.*, **1195**, 877 (2019); https://doi.org/10.1016/j.molstruc.2019.06.042
4. Z.D. Petrovic, J. Dorovic, D. Simijonovic, V.P. Petrovic and Z. Markovic, *RSC Adv.*, **5**, 24094 (2015); https://doi.org/10.1039/C5RA02134K
5. A.M. Abu-Dief and I.M.A. Mohamed, *Beni Suef Univ. J. Basic Appl. Sci.*, **4**, 119 (2015); https://doi.org/10.1016/j.bjbas.2015.05.004
6. S.N. Mbugua, N.R.S. Sibuyi, L.W. Njenga, R.A. Odhiambo, S.O. Wandiga, M. Meyer, R.A. Lalancette and M.O. Onani, *ACS Omega*, **5**, 14942 (2020); https://doi.org/10.1021/acsomega.0c00360
7. S. Layek, B. Anuradha, B. Agrahari and D. Pathak, *J. Organomet. Chem.*, **846**, 105 (2017); https://doi.org/10.1016/j.jorganchem.2017.05.049

8. P. Tyagi, M. Tyagi, S. Agrawal, S. Chandra, H. Ojha and M. Pathak, *Spectrochim. Acta A Mol. Biomol. Spectrosc.*, **171**, 246 (2017); https://doi.org/10.1016/j.saa.2016.08.008
9. N. Fahmi, S. Shrivastava, R. Meena, S.C. Joshi and R.V. Singh, *New J. Chem.*, **37**, 1445 (2013); https://doi.org/10.1039/c3nj40907d
10. M. Manjunath, A.D. Kulkarni, G.B. Bagihalli, S. Malladi and S.A. Patil, *J. Mol. Struct.*, **1127**, 314 (2017); https://doi.org/10.1016/j.molstruc.2016.07.123
11. M. Fuentealba, J.-R. Hamon, D. Carrillo and C. Manzur, *New J. Chem.*, **31**, 1815 (2007); https://doi.org/10.1039/b707934f
12. M.A.-A.A.A. Islam, M.T.H. Tarafder, M.C. Sheikh, M.A. Alam and E. Zangrando, *Transition Met. Chem.*, **36**, 531 (2011); https://doi.org/10.1007/s11243-011-9499-6
13. M.H.E. Chan, K.A. Crouse, M.I.M. Tahir, R. Rosli, N. Umar-Tsafe and A.R. Cowley, *Polyhedron*, **27**, 1141 (2008); https://doi.org/10.1016/j.poly.2007.11.035
14. S. Sharma, R. Meena, Y. Satyawana and N. Fahmi, *Russ. J. Gen. Chem.*, **86**, 2807 (2016); https://doi.org/10.1134/S1070363216120446
15. M.T.H. Tarafder, A. Asmadi, S.M.S. Talib, A.M. Ali and K.A. Crouse, *Transition Met. Chem.*, **26**, 170 (2001); https://doi.org/10.1023/A:1007119504397
16. F.N.F. How, K.A. Crouse, M.I.M. Tahir, M.T.H. Tarafder and A.R. Cowley, *Polyhedron*, **27**, 3325 (2008); https://doi.org/10.1016/j.poly.2008.07.022
17. H. Brahim, *J. Lumin.*, **210**, 96 (2019); https://doi.org/10.1016/j.jlumin.2019.02.030
18. Y. Kim, J. Lee, Y. Son, S. Unchoi, M. Alam and S. Park, *J. Inorg. Biochem.*, **205**, 111015 (2020); https://doi.org/10.1016/j.jinorgbio.2020.111015
19. M.A. Arafath, F. Adam, M.R. Razali, L.E.A. Hassan, M.B.K. Ahamed and A.M.S. Majid, *J. Mol. Struct.*, **1130**, 791 (2017); https://doi.org/10.1016/j.molstruc.2016.10.099
20. A. Bouchoucha, S. Zaater, S. Bouacida, H. Merazig and S. Djabbar, *J. Mol. Struct.*, **1161**, 345 (2018); https://doi.org/10.1016/j.molstruc.2018.02.057
21. E. Pahontu, S. Shova, G. Lupascu, D.C. Ilies, S.F. Barbuceanu, L.I. Socea, M. Badea, V. Pãunescu, D. Istrati, A. Gulea, D. Draganescu and C.E. Dinu Pirvu, *Appl. Organomet. Chem.*, **33**, 5185 (2019); https://doi.org/10.1002/aoc.5185
22. A.K.S. Pereira, C.M. Manzano, D.H. Nakahata, J.C.T. Clavijo, D.H. Pereira, W.R. Lustri and P.P. Corbi, *New J. Chem.*, **44**, 11546 (2020); https://doi.org/10.1039/D0NJ02009E
23. A.I. Vogel, A Textbook of Quantitative Chemical Analysis, 6th Edition. Pearson Education Ltd.: UK, pp. 387-498 (2006).
24. N. Fahmi, R. Meena, P. Mitharwal, S. Shrivastava and R.V. Singh, *Int. J. Pharma Sci.*, **5**, 2821 (2014).
25. A. Kumari, R. Meena, R.V. Singh and N. Fahmi, *Indian J. Chem.*, **60A**, 341 (2021).
26. K. Sharma, M. Swami, R. Singh, N. Fahmi and R.V. Singh, *Phosphorus Sulfur Silicon Rel. Elem.*, **184**, 1964 (2009); https://doi.org/10.1080/10426500802417133